Prediction of High Level Vibration Test Results by Use of Available Inelastic Analysis Techniques

C. H. HOFMAYER, Y. J. PARK
Brookhaven National Laboratory, Upton, NY USA
J. F. COSTELLO
U. S. Nuclear Regulatory Commission, Washington, DC USA

1 INTRODUCTION

As part of a cooperative study between the United States and Japan, the U.S. Nuclear Regulatory Commission (USNRC) and the Ministry of International Trade and Industry (MITI) of Japan agreed to perform a test program that would subject a large scale piping model to significant plastic strains under excitation conditions much greater than the design condition for nuclear power plants. The objective was to compare the results of the tests with state-of-the-art analyses. Comparisons were done at different excitation levels from elastic to elastic-plastic to levels where cracking was induced in the test model. The program was called the High Level Vibration Test (HLVT) and was described in the 10th SMiRT Proceedings (Kawakami et al 1989 and Hofmayer et al 1989). A complete description of the test results and the pre- and post-test analyses performed by Brookhaven National Laboratory (BNL) are contained in NUREG/CR-5585 (Park et al 1991). Other post-test predictions sponsored by USNRC/BNL were performed by Westinghouse Electric Corporation, ABB Impell Corporation and Structural Analysis Technologies (SAT), Inc. This paper will summarize the post-test analysis efforts by BNL and the above organizations and present comparisons with the test results. The Electric Power Research Institute (EPRI), one of the sponsors of the testing, also conducted a post-test prediction project. Their results are described in another paper in the 11th SMiRT Proceedings (Jaquay et al 1991).

2 SUMMARY OF HLVT RESULTS

The HLVT was performed on the seismic table at the Tadotsu Engineering Laboratory of Nuclear Power Engineering Test Center (NUPEC) in Japan. The test model was constructed by modifying the 1/2.5 scale model of one loop of a PWR primary coolant system which was previously tested by NUPEC as part of their seismic proving test program. An isometric view of the test model and support frame is shown in Figure 1. The input motion applied to the vibration table consisted of a modified earthquake excitation which was increased up to the limit of the table so as to induce inelastic response in the model. A number of test runs were performed, many consisting of four segments of random motion lasting about 40 seconds. The amplitude of the applied loading varied from cycle to cycle in each run and the peak loading increased progressively throughout the initial test runs. A complete description of the excitation procedure was presented in the 10th SMiRT Proceedings (Kawakami, et al 1989). During the early test runs the model's response was mainly elastic. For the

intermediate test runs the input motion was increased and plasticity was observed in the test model. For the highest test runs the input motion was scaled up to the capacity of the vibration table. The final test run was terminated after applying one segment of the motion which lasted about 10 seconds. During the vibration tests the piping was subjected to an internal pressure of 1.57 Kgf/mm^2 (2.23ksi) and maintained at that pressure throughout the test.

Post-test examinations of the HLVT model have shown that bulging due to fatigue ratchetting occurred in the hot leg pipe at two locations, one near the "vessel" attachment point and one near the elbow that was attached to the "steam generator." The bulging near the elbow was more pronounced than that near the vessel attachment. However, neither of these bulges resulted in failure of the piping system. Rather, a circumferential fatigue crack initiated in the hot leg elbow near its attachment weld to the hot leg straight pipe. Figure 2 illustrates the location of the bulging and cracking in the hot leg pipe. The length of the crack along the surface of the pipe and its depth were measured after each load sequence. The maximum crack depth penetrated up to 94% of the wall thickness and the crack extended over approximately 31% of the pipe circumference.

3 POST-TEST ANALYSIS

For the pre-test analysis inelastic dynamic analyses were performed by BNL using the MARC Code (Hofmayer et al 1991). The straight pipe segments of the test model were represented by pipe elements and the five elbows in the test model were represented by elbow elements. In addition to the MARC Code, BNL used the ABAQUS Code in the post-test analysis phase to compare time history responses using different computer codes. For the ABAQUS model the two-node elbow element, "ELBOW 31," was used for straight pipes, and the three-node elbow element, "ELBOW 32," was used for pipe bends. The overall arrangement of the ABAQUS model is shown in Figure 3. This model is the same as that used for the MARC model, except for the piping modeling and a few details reflecting differences in codes.

The piping of the test model, especially the elbows, is of a relatively thick-wall design. The piping modeling of the foregoing analysis models, however, are based on thin-wall shell assumptions. An additional analysis model was developed to obtain responses without the shell-type deformation of piping in order to compare with the foregoing models. The above ABAQUS elbow model was modified for this purpose by replacing the elbow elements, "ELBOW 31" and "ELBOW 32," by nonlinear beam elements, "B31" and "B32," respectively. Therefore, in this modeling, the effect of the internal pressure is not included.

For the MARC analysis a multi-linear curve was used to model the stress-strain relationship of the stainless steel virgin material used for the piping. In using the ABAQUS Code, however, a bilinear curve is used for the same material since it is the only available option. In using both the MARC and ABAQUS Codes, the kinematic hardening rule was used to prescribe the hysteretic behavior of the material. Since the kinematic hardening rule is "history-independent," the effect of previous loadings could not be incorporated in the analyses. Therefore, each analysis was performed as an isolated run. However, additional ABAQUS analyses were performed with the yield stress increased by approximately 30 percent to account for the yield stress increase due to prior runs. This yield stress increase was observed in post-test tensile tests of material removed from the bulged region of the hot leg pipe. In subsequent discussions the ABAQUS elbow and beam models which utilize the virgin material yield stress are referred to as ELBOW-A and

BEAM-A. The models which utilize a 30 percent increase in yield stress are referred to as ELBOW-B and BEAM-B.

In addition to the BNL analyses, other organizations using different inelastic analysis techniques performed post-test analyses of the HLVT model. Each organization was given sufficient information to develop an analytical model similar to that shown in Figure 3. They were then requested to make analytical predictions given the first segment of the acceleration time history recorded at the Maximum Plastic Run (MPR) test level, as well as two lower test levels (0.1 MPR and 0.4 MPR). The peak accelerations for these three time histories were 185, 1099 and 2310 gals. Initial predictions were made without knowledge of the test results. Then each organization was given an opportunity to reconcile their predictions with the test results. The results from their final predictions are presented in this paper.

Westinghouse developed a detailed finite element system model using the WECAN Code. The model consisted of three dimensional elastic or elastic-plastic pipe elements (either straight or curved) to represent the loop piping and the equipment components. Elbow flexibility values were used based on test data for an elbow similar to that in the HLVT. A multilinear combined kinematic-isotropic hardening rule was used. A static component model consisting of 3-D isoparametric solid elements was developed for the hot leg elbow region to account for local effects such as ovalization, stress concentrations and through wall stress variations.

Impell also developed a detailed finite element model using the ADINA Code. The piping was modeled with nonlinear elements while the remainder of the structure utilized linear elements. The elbows utilized four-node elbow elements in which the ovalization varies cubically along its length. A similar element was utilized to model a small straight pipe segment adjacent to the hot leg elbow. The remaining straight pipe segments were modeled with two-node elements without consideration for ovalization. A kinematic strain hardening rule was used. In subsequent discussions this model is referred to as Impell-B.

In addition to the above detailed analyses, Impell and SAT utilized simplified analysis techniques. The Impell approach uses both the Spectral Averaging (SA) and Riddell-Newmark (RN) ductility modified response spectrum techniques (Wesley 1991). In subsequent discussions the results from the SA method are referred to as Impell-A. The simplified analysis method developed by SAT also uses a response spectrum approach which employs local ductilities and modified ductility ratios based on ratchetting behavior.

4 COMPARISON WITH TEST RESULTS

Figures 5 and 6 illustrate the test results for the peak displacements and accelerations of the top of the steam generator (SG) for all test runs. The analysis predictions bracket the test results fairly well in the loading direction. However, the SG response in the orthogonal (Y) direction, which may have been significantly affected by the existance of gaps in the lower SG pin connection, is not reproduced properly by the analyses. Also, as illustrated in Figure 7, for the peak shear force at the SG pin connection the predicted results for 1.0 MPR were 30 to 60 percent below the measured values. As can be seen, after modifications to the SG support, the differences between the measured and predicted forces increased.

Figure 8 compares the measured axial strain distribution along the hot leg pipe with the analysis results from ABAQUS (Elbow-B), WECAN and ADINA. The overall pattern of the strain distribution is captured; however, there are substantial variations in the ability to predict the strain at specific locations. Figure 9 illustrates the percentage error observed for the various

analysis models. At the 0.1 MPR level (limit of elastic response), the overall response predictions are quite good; however, the strains in general were predicted well in some case and underpredicted by as much as 60 percent in other cases. (Note: no comparisons for the SG pin force are made at 0.1 MPR). At the 1.0 MPR level the variation in strain predictions become much larger, but again there are cases of good correspondence. As illustrated in Figure 9(c), the use of a higher yield stress and the beam model tends to improve the strain prediction in the highly plastic region.

Figure 10 illustrates the time history of the measured axial strain at the center top part of the hot leg elbow. The corresponding prediction by ABAQUS ELBOW-B is shown in Figure 11. As can be seen a significant strain ratchet effect is predicted which was not observed in the test results. The ABAQUS ELBOW-B time history of hoop strain is shown in Figure 12. Again, a significant ratchet strain is predicted which was not observed in the test. The test strain time history is not shown, but the pattern is similar to Figure 10. The results for the other analysis codes considered in the program also predict strain ratchetting which was not observed in the tests. This ratchetting tendency was found to be sensitive to the assumed yield stress level.

5 CONCLUSIONS

A comparison of various analysis techniques with test results shows a higher prediction error in the detailed strain values than in the overall response values. This prediction error is magnified as the plasticity in the test model increases. There is no significant difference in the peak responses between the simplified (i.e., SAT and IMPELL-A) and the detailed analyses. A comparison between various detailed finite element model runs indicates that the material properties and plasticity modeling have a significant impact on the plastic strain responses under dynamic loading reversals.

REFERENCES

Hofmayer, C. et al (1989). High Level Vibration Test of Nuclear Power Piping - Overall Plan, Input Motion Development and Analysis, Volume S, 10th SMiRT, pp. 93-98.

Jaquay, K.R., Quiñones, D.F., and Tang, H.T. (1991), Post-Test Predictions of High Level Vibration Tests of Nuclear Piping, Volume K, 11th SMiRT.

Kawakami, S. et al (1989). High Level Vibration Test of Nuclear Power Piping - Test Procedures and Test Results, Volume K2, 10th SMiRT, pp. 745-750.

Park, Y.J., Curreri, J.R., and Hofmayer C.H. (1991). The High Level Vibration Test Program Final Report, USNRC NUREG/CR-5585.

Wesley, D.A. (1991), Ductility-Modified Response Spectra Methods for Ductile Equipment Seismic Failure Analysis, Volume K, 11th SMiRT.

ACKNOWLEDGEMENTS

This work was performed as part of the HLVT post-test prediction program conducted by BNL for the USNRC. The principal investigators for the other organizations who participated in this program are T.H. Liu of Westinghouse, W.F. Hahn and D.A. Wesley of ABB Impell, and H. Kamil of SAT.

The HLVT project was performed by BNL and NUPEC as part of a nuclear power technical cooperative agreement between the USNRC and MITI in Japan. The authors wish to thank S. Kawakami, N. Tanaka, K. Koyama, as well as the many other members of the NUPEC and Mitsubishi staff who contributed to the successful completion of this project.

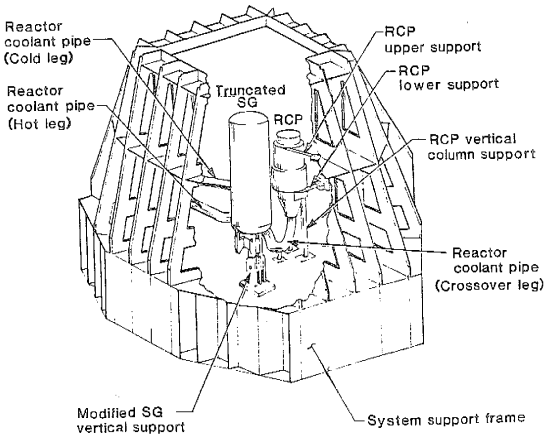

Figure 1 HLVT Model

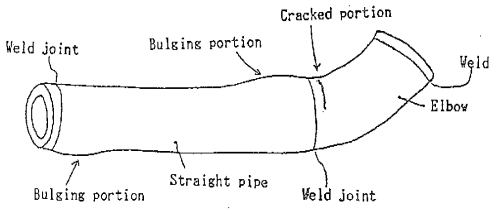

Figure 2 Hot Leg Pipe

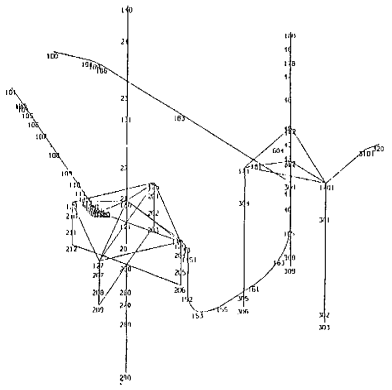

Figure 3 ABAQUS Model

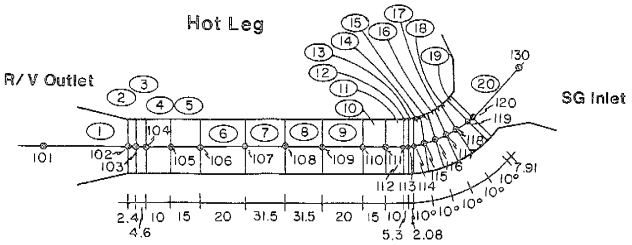

Figure 4 ABAQUS Hot Leg Model

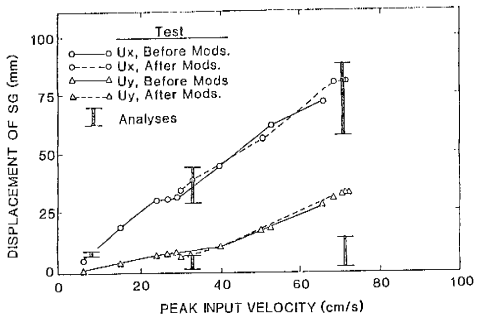

Figure 5 Peak Displacement of Steam Generator

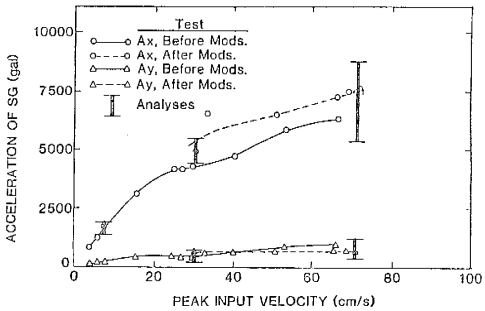

Figure 6 Peak Acceleration of Steam Generator

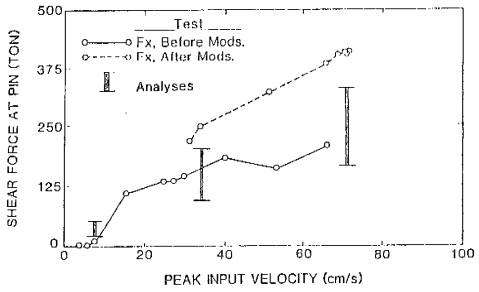

Figure 7 Peak Shear Force at SG-Pin Connection

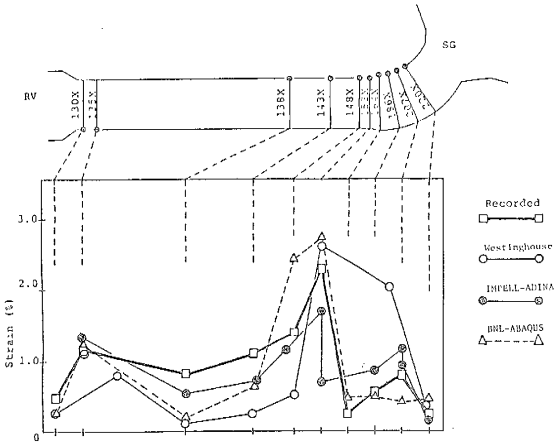

Figure 8 Axial Strain Distribution at 1.0 MPR (A-Segment)

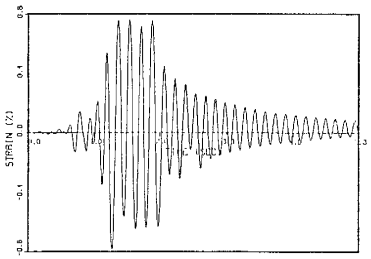

Figure 10 Axial Strain Measured in Elbow at 207X (1.0MPR)

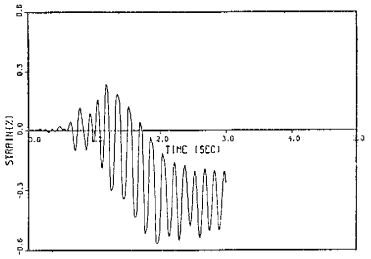

Figure 11 ABAQUS Predicted Axial Strain in Elbow at 207X (1.0 MPR)

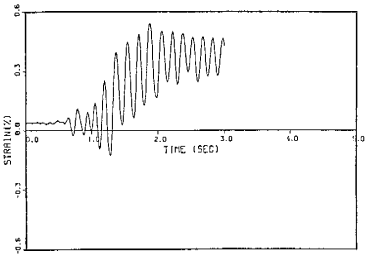

Figure 12 ABAQUS Predicted Hoop Strain in Elbow at 207Y (1.0MPR)

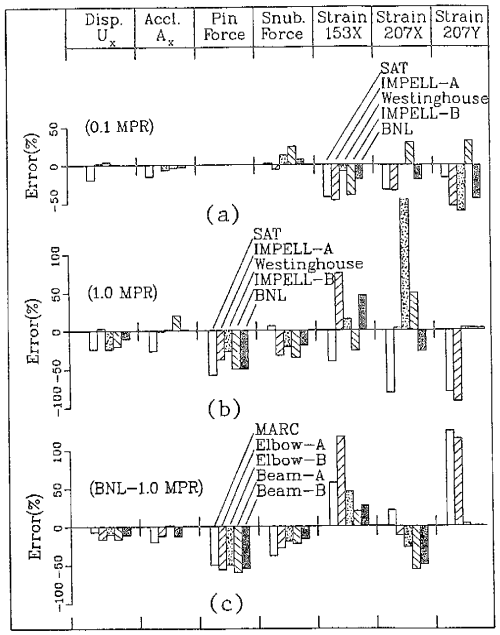

Figure 9 Comparison of Analyses with Test Results